Simulation of entanglement generation and variation in quantum computation

Ioannis G. Karafyllidis *

Department of Electrical and Computer Engineering, Democritus University of Thrace, 671 00 Xanthi, Greece

Abstract

Entanglement generation and variation in quantum computation is studied using a quantum computer simulator. The simulator is described and its block diagram is presented. The use of this simulator allows the study of entanglement manipulation in quantum computations that comprise more than two qubits and a variety of quantum gates such as Hadamard, Controlled-Not, Controlled-controlled-Not, Controlled-phase and Fredkin gates. Simulations of entanglement variation in four-qubit and six-qubit quantum Fourier transforms with entangled initial states is also studied.
© 2004 Elsevier Inc. All rights reserved.

Keywords: Quantum computation; Entanglement; Simulation

1. Introduction

Entanglement is an enigmatic feature of the formalism of quantum mechanics with no classical analogue. Its importance was firstly considered in the paradox proposed by Einstein, Podolsky and Rosen, known as the EPR paradox [1] and it manifests itself in strong non-local correlations of measurement outcomes.The renewed interest in the study of entanglement is largely due to the fact that entanglement plays a key role in quantum information processing [2,3]. Entanglement is a physical resource and can be defined as the potential of quantum states, that describe particles that have interacted in the past but are presently non-interacting, to exhibit strong correlations that cannot be accounted for classically [4,5]. Entanglement is the key feature of the most successful quantum algorithm, namely Shor's quantum algorithm for factoring a large integer [6]. Understanding all the aspects of entanglement is expected to lead to the development of new quantum algorithms [7].

* Tel.: +30-541-79548; fax: +30-541-29647.
E-mail address: ykar@ee.duth.gr (I.G. Karafyllidis).
URL: http://vlsi.ee.duth.gr/~ykar.

One of the major challenges in quantum computation is the characterization of entanglement. This characterization has three aspects: the qualification of entanglement (i.e., to determine if a given state is entangled or not), the quantification of entanglement (i.e., to calculate the amount of entanglement of an entangled state) and the manipulation of entanglement (i.e., to predict and control the generation and variation of entanglement in quantum computations) [8,9]. The research work described in this paper deals with manipulation of entanglement.

Studies of entanglement generation and variation in two-quantum bit (qubit) systems have been recently presented in the literature [10–12]. In this paper the entanglement generation and variation is studied using a quantum computer simulator. This simulator was developed by the author and has been used for the visualization of the quantum Fourier transform [13] and for the simulation of cellular quantum computer architecture [14]. The simulator has been extended in order to include calculations and graphical representations of entanglement generation and variation in quantum computations. The use of this simulator allows the study of entanglement manipulation in quantum computations that comprise more than two qubits and a variety of quantum gates. Simulation results of entanglement generation and variation in quantum computations that comprise four and six qubits are presented in this paper. These quantum computations comprise Hadamard (H), Controlled-Not (CN), Controlled-controlled-Not (CCN), Controlled-phase (CP) and Fredkin (F) quantum gates. Simulation results of entanglement variation in four-qubit and six-qubit quantum Fourier transform are also presented. The results show that manipulation of entanglement in n-qubit computations with the aid of a quantum computer simulator is possible and may help researches to develop new quantum algorithms.

2. Entanglement measure

In error-free quantum computations the quantum register (QR) is found in pure states. The qubits of the QR are in a pure but non-factorisable state. For any bipartite system it has been shown that the entanglement of the system can be defined as the von Neumann entropy of either of its two parts [4,5]. A pure state is entangled if and only if its state vector $|\psi\rangle$ cannot be expressed as a tensor product of pure states of its parts, $|\psi_A\rangle$ and $|\psi_B\rangle$

$$|\psi\rangle \neq |\psi_A\rangle \otimes |\psi_B\rangle. \tag{1}$$

A pure state's entanglement is measured by its entropy of entanglement

$$E(\psi) = S(\rho_A) = S(\rho_B), \tag{2}$$

i.e., the apparent entropy of either subsystem [4,5]. In Eq. (2) $S(\rho)$ is the von Neumann entropy given by

$$S(\rho_A) = -\text{Tr}(\rho_A \log_2 \rho_A),$$
$$S(\rho_B) = -\text{Tr}(\rho_B \log_2 \rho_B), \tag{3}$$

where ρ_A and ρ_B are the reduced density matrices obtained as partial traces of the whole system's pure density matrix $\rho = |\psi\rangle\langle\psi|$ over the two subsystems:

$$\rho_A = \text{Tr}_B(|\psi\rangle\langle\psi|),$$
$$\rho_B = \text{Tr}_A(|\psi\rangle\langle\psi|). \tag{4}$$

In terms of the eigenvalues $\{\lambda_i\}$ of the density matrix ρ the von Neumann entropy is given by [4,5]

$$S(\rho) = -\text{Tr}(\rho \log_2 \rho) = \sum_i -\lambda_i \log_2 \lambda_i. \tag{5}$$

The entanglement E is measured in entangled bits (ebits), which are defined as the amount of entanglement in a maximally entangled state of any pure bipartite system for which $E = 1$. In the case of a quantum register that comprises n qubits the system can be divided into two parts: the qubit j and the rest of the quantum register now comprising $n - 1$ qubits. In this case the entanglement is obtained as described
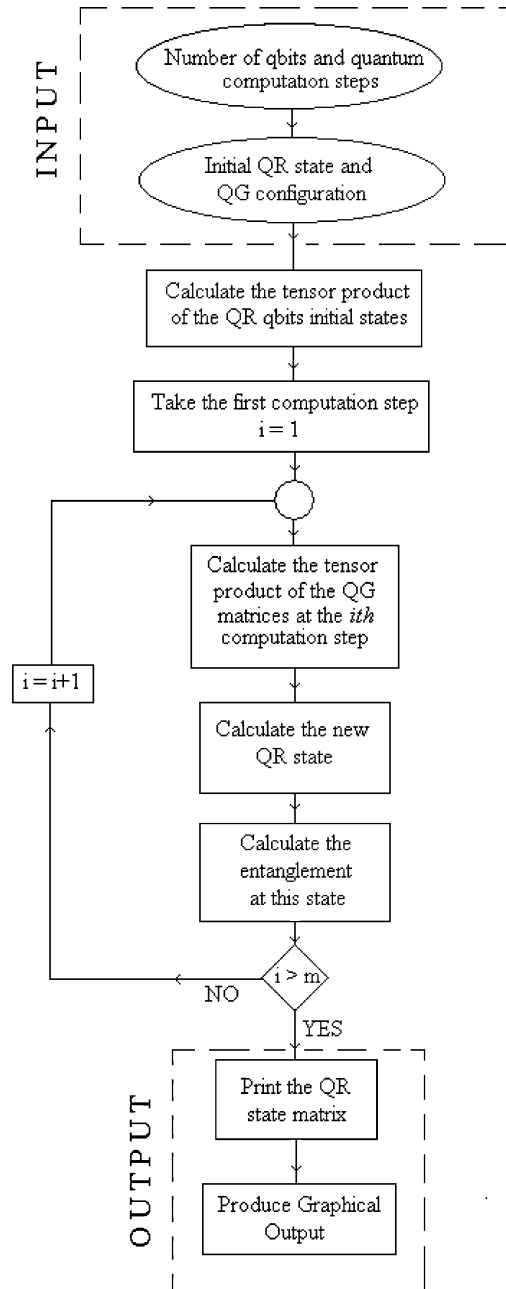

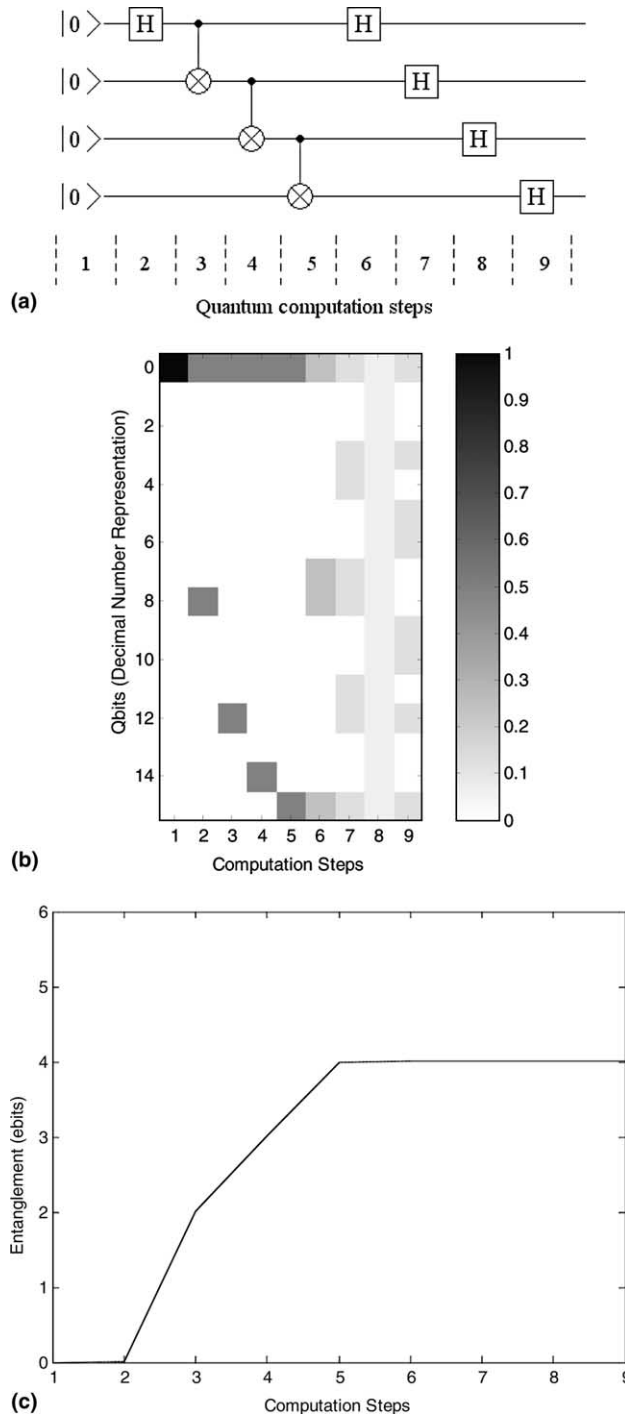Fig. 1. The block diagram of the quantum computer simulator.

Fig. 2. (a) The quantum circuit for the production of a four-qubit GHZ state, followed by four H gates. (b) The simulation of this quantum computation. (c) Entanglement variation for this quantum computation.
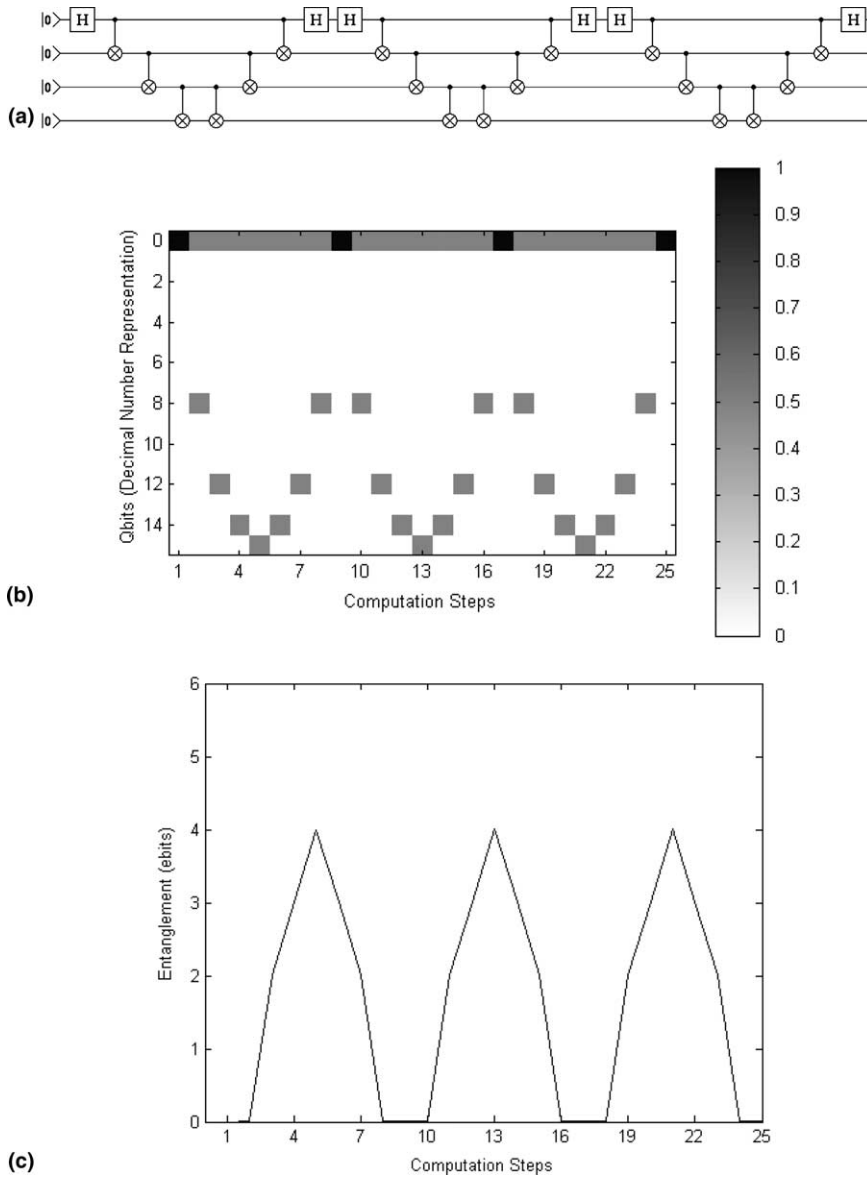
Fig. 3. (a) A quantum computation with a configuration of quantum gates applied three times. The configuration starts with an H gate applied to the first qubit followed by six CN gates and ends with an H gate applied again to the first qubit. (b) The simulation of this quantum computation. (c) Entanglement variation for this quantum computation.

above. A more indicative measure of entanglement is the sum of the entanglements calculated by considering each qubit as one of the parts and the rest qubits as the other part

$$E = \sum_{j=1}^{n} S(\rho_j) = \sum_{j=1}^{n} -\mathrm{Tr}(\rho_j \log_2 \rho_j). \tag{6}$$
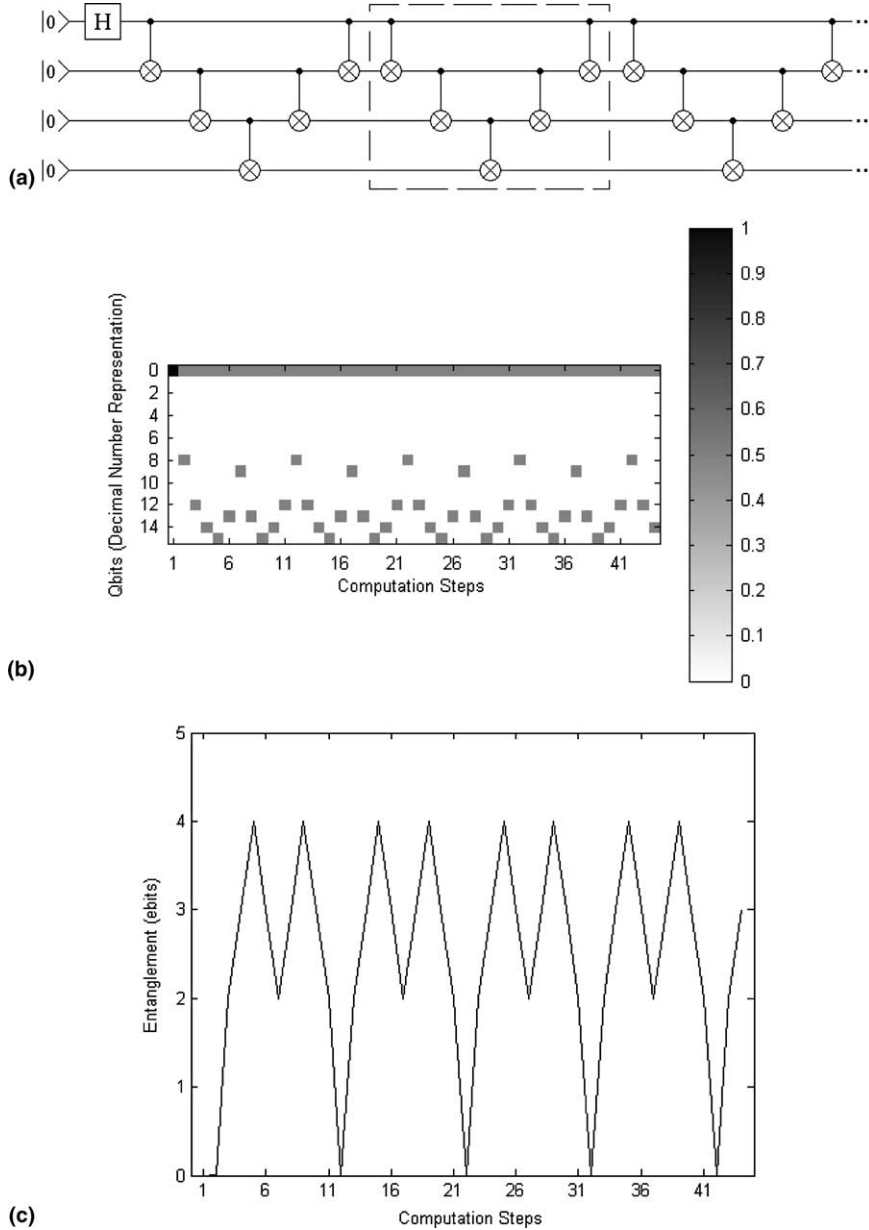
Fig. 4. (a) A quantum computation where after the application of an H gate to the first qubit, the quantum gate configuration enclosed in the dashed rectangle is applied nine times. (b) The simulation of this quantum computation. (c) Entanglement variation for this quantum computation.

Using (6) the entanglement of a quantum register with n qubits, four of which are fully entangled is 4. Eqs. (1)–(6) are used for the calculation of entanglement in the quantum computer simulator presented in the next section. It must be emphasized that Eq. (6) is not a measure of entanglement of the multipartite state represented by the QR. It is the sum of bipartite entanglements between each qubit and the rest of the QR.

3. The quantum computer simulator

The block diagram of the quantum computer simulator is shown in Fig. 1. The inputs to the simulator are the initial state of the qubits that form a QR and the gates applied at each computation step.

The user of the simulator is asked to enter the number of the qubits in the QR and the number of computation steps. The initial state of the QR is entered as a one-dimensional matrix, the elements of which are 0 and 1. The gate configuration is entered as a two-dimensional matrix. The element $QG_{i,j}$ represents the ith gate applied at the jth computation step. The elements of the matrix $[QG]$ are 0, 1, 2, 3, 4, 5, 6 and 9. The H, Φ, CN, CCN, F and $C\Phi$ gates are represented by 1, 2, 3, 4, 5 and 6, respectively. The digit 0 represents the identity operator. $QG_{i,j} = 0$ means that no gate is applied at the ith qubit at the jth computation step. "No gate is applied" is significant in quantum computation and is represented by the 2×2 identity matrix, and contributes to the gate tensor product at this step. The digit 9 is used to denote a controlling qubit. For example the part of $[QG]$ representing the application of a two-input CN gate followed by a three-input CCN gate is

$$\begin{bmatrix} \cdots & \cdots & \cdots & \cdots \\ \cdots & 9 & 9 & \cdots \\ \cdots & 3 & 9 & \cdots \\ \cdots & \cdots & 4 & \cdots \\ \cdots & \cdots & \cdots & \cdots \end{bmatrix}. \tag{7}$$

In the case where the controlling qubits and the controlled qubit are not in sequence at some computation step, a virtual gate, the swap gate, is used to change the order of qubit lines for that particular step.

After the inputs are entered, the tensor product of the initial state of the QR is calculated. Then, the simulator enters the loop. The tensor product of the gate matrices applied at the first step is calculated. After that, the new state of the QR is calculated. Next, the measure of entanglement of the new QR state is calculated using Eqs. (1)–(6). The new state of the QR is used as the initial state in the next iteration. The tensor product of the gate matrices applied at the second iteration is calculated and after that the new QR state, the entanglement measure, and so on until the number of iterations, set by the user, is reached.

After the end of the calculation the simulator apart from the matrices that represent the QR state at each quantum computation step and the entanglement measure calculated for the QR states at all quantum computation steps, produces two graphical outputs. The first comprises the probability of measuring each one of the possible final QR states. This graphical output displays the evolution of the QR states during all computation steps. The probability is represented as a gray-scale image in which probability 1 is represented by black and probability 0 by white. The second graphical output displays the entanglement measure calculated at each quantum computation step.

The computational complexity of any algorithm simulating quantum systems with two base states is $O(2^n)$, where n is the number of quantum systems with two base states. This simulator is no exception to
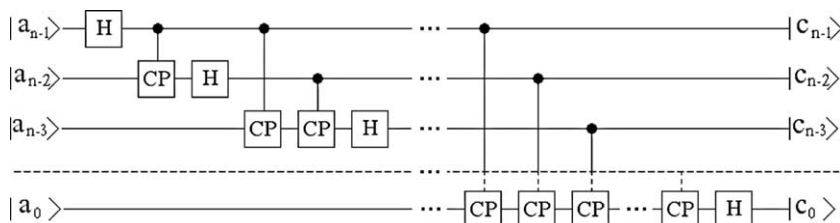

Fig. 5. The quantum circuit that executes the quantum Fourier transform.

that and suffers from exponential slowdown as the number of qubits increases. Fortunately, the matrices representing qubits and quantum gates contain a large number of zeros and the computation complexity can be improved using sparse matrix techniques. Special attention has been given not to include many
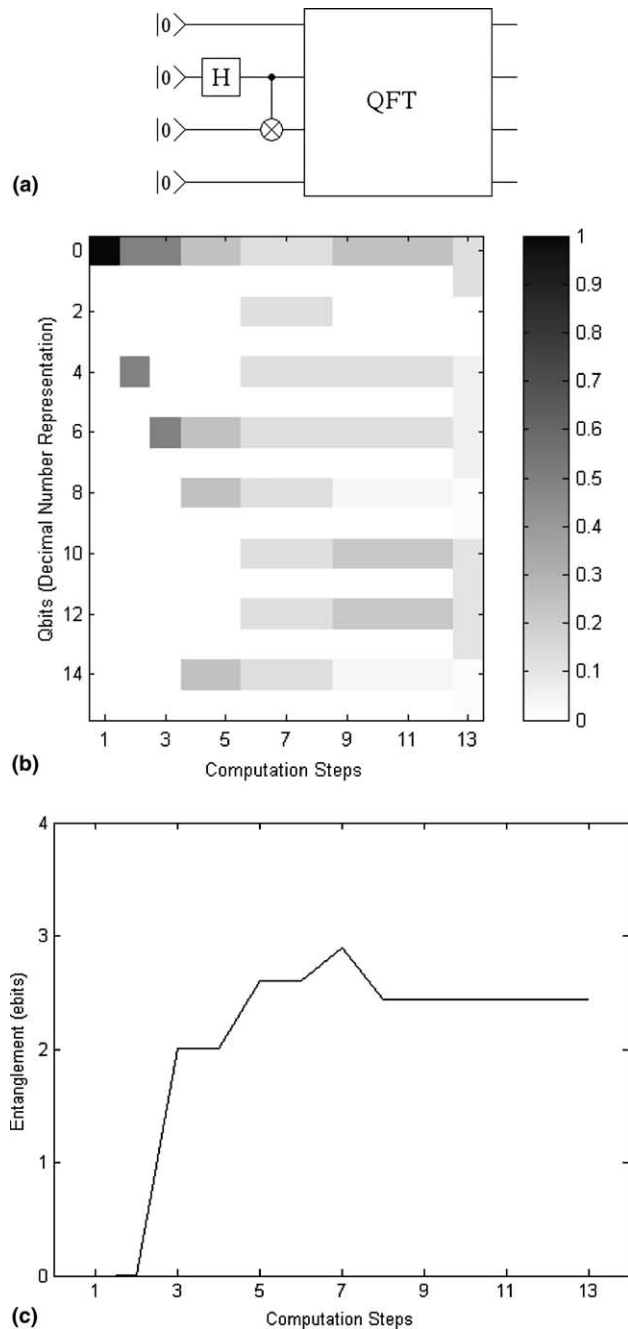

Fig. 6. (a) A quantum computation where the second and third qubits are entangled and then the four-qubit QFT circuit is applied. (b) The simulation of this quantum computation. (c) Entanglement variation for this quantum computation.
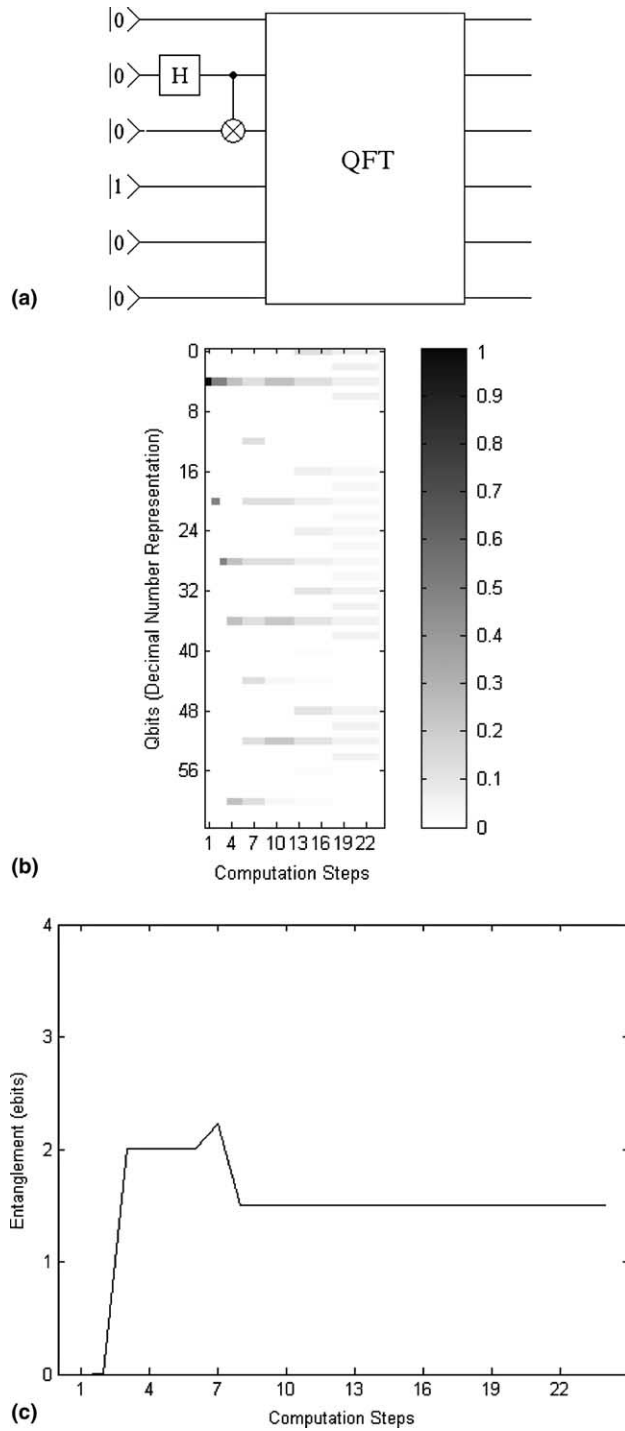
Fig. 7. (a) A quantum computation where the second and third qubits are entangled and then the six-qubit QFT circuit is applied. (b) The simulation of this quantum computation. (c) Entanglement variation for this quantum computation.

decision points (*if* statements) into the simulator. It can be seen from the simulator block diagram, that only one decision point is used, allowing thus the simulation of quantum computations with several qubits.

4. Simulations of entanglement generation and variation

Simulations of entanglement generation and variation in several quantum computations will be presented in this section. The first quantum computation simulated is the production of GHZ states, which are maximally entangled. Fig. 2(a) shows the quantum circuit for the production of a four-qubit GHZ state. In this figure the quantum computation steps are numbered. The first step corresponds to the initial state of the four-qubit QR. The circuit comprises an H gate followed by CN gates acting on neighboring qubits. At the fifth computation step four H gates are applied, one at each computation step. Fig. 2(b) shows the simulation of this quantum computation. On the *y*-axis the states are represented by the decimal numbers corresponding to the binary numbers that label each state. The *x*-axis gives the number of the computation step. The probability to measure a state at each computation step is shown as a gray-scale image in which 1 is represented by black and 0 by white. The initial state is represented by decimal 0 and is shown in black since its probability at the first computation step is 1. Fig. 2(c) shows the entanglement variation for this computation in ebits. The *y*-axis is the calculated entanglement measure at each computation step according to Eqs. (1)–(6) and the *x*-axis numbers the computation steps. As expected entanglement is
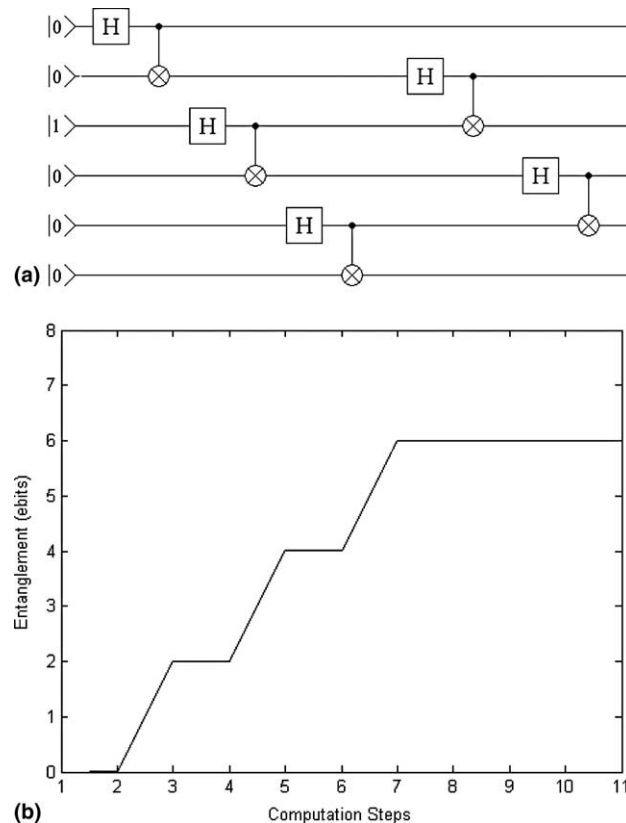

Fig. 8. (a) An entangled chain of six qubits. (b) Entanglement variation.

generated after the application of the first CN gate and increases by one ebit each time a CN gate is applied, because one more qubit becomes entangled. Entanglement reaches its maximum value (4 ebits) after the application of the third CN gate. At this computation step all four qubits are fully entangled. As expected, the following application of H gates does not change the entanglement.

4.1. Repeated applications of the same quantum gate configurations

The second computation is represented by the quantum circuit of Fig. 3(a), where the same configuration of quantum gates is applied three times. The repeated configuration starts with an H gate applied to the first qubit followed by six CN gates and ends with an H gate applied again to the first qubit. Fig. 3(b) shows the simulation of this quantum computation. The initial state is represented by decimal 0 and is shown in black. Fig. 3(c) shows the entanglement variation for this computation. Entanglement is generated after the application of the first CN gate, increases by one ebit each time a CN gate is applied and reaches its maximum value (4 ebits) after the application of the third CN gate. The application of the fifth and sixth CN gates followed by an H gate applied to the first qubit, fully disentangles the QR and the entanglement is now zero ebits. The application of the same quantum gate configuration two more times results in the same entanglement variation.

A similar quantum computation is shown in Fig. 4(a) where, after the application of an H gate, which sets in base-state superposition the first qubit, the quantum gate configuration enclosed in the dashed
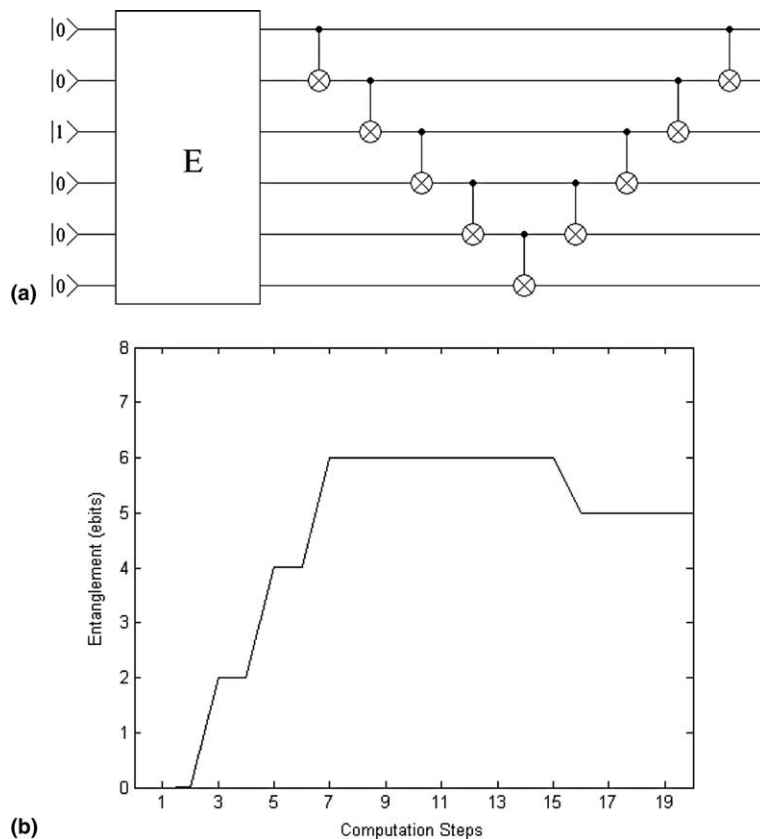

Fig. 9. (a) An entangled chain of six qubits followed by CN gates. (b) Entanglement variation.

rectangle is applied nine times. The simulation of this computation is shown in Fig. 4(b) and the entanglement variation in Fig. 4(c). As shown in Fig. 4(c) entanglement is generated, the state of the QR becomes fully entangled, then partially disentangled and then fully entangled again. The same variation is repeated nine times. Quantum computations of Figs. 3 and 4 indicate that it may be possible to produce periodic entanglement variation by applying repeatedly the same quantum gate configuration. This fact may lead to useful quantum computations and even in new quantum algorithms.

4.2. Entanglement variation by the quantum Fourier transform

Next, the entanglement variation during the quantum Fourier transform (QFT) is studied using the quantum computer simulator. The QFT is a key subroutine of quantum algorithms for factoring and quantum simulations and is the heart of the hidden-subgroup problem, the solution of which is expected to lead to the development of new quantum algorithms [15]. The QFT has been extensively studied [16] and has also been implemented on a nuclear magnetic resonance (NMR) quantum computer [17].

The QFT is a unitary operation that acts on vectors in the Hilbert space. QFT acts on a base state of the N-dimensional Hilbert space as follows [18]:

$$\mathrm{QFT}_N : |a\rangle \mapsto \frac{1}{\sqrt{N}} \sum_{c=0}^{N-1} \mathrm{e}^{2\pi \mathrm{i} \frac{ac}{N}} |c\rangle, \tag{8}$$

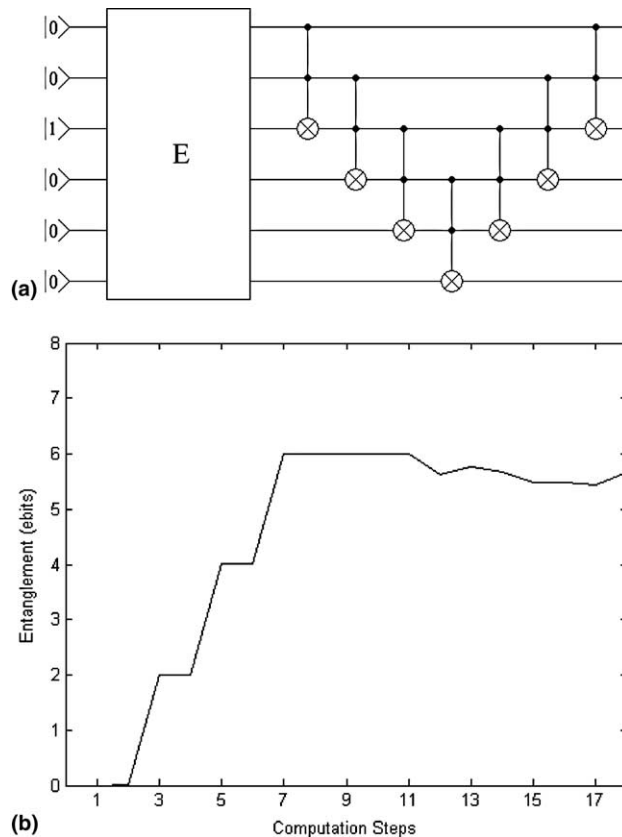
Fig. 10. (a) An entangled chain of six qubits followed by CCN gates. (b) Entanglement variation.

where QFT$_N$ is the symbol of the QFT on the N-dimensional Hilbert space, $|a\rangle$ and $|c\rangle$ are base states in decimal representation and (ac) is the ordinary multiplication of the two decimal numbers a and c. Any state vector in the N-dimensional Hilbert space can be expressed as a superposition of base states and QFT transforms it according to

$$\text{QFT}_N : \sum_{a=0}^{N-1} x_a|a\rangle \mapsto \frac{1}{\sqrt{N}} \sum_{c=0}^{N-1} \sum_{a=0}^{N-1} x_a e^{2\pi i\frac{ac}{N}}|c\rangle = \frac{1}{\sqrt{N}} \sum_{c=0}^{N-1} y_c|c\rangle, \tag{9}$$

where y_c is the classical discrete Fourier transform (DFT) of x_a

$$\text{DFT}_N : y_c \mapsto \sum_{a=0}^{N-1} e^{2\pi i\frac{ac}{N}} x_a. \tag{10}$$

QFT is a unitary operator which is used to force interference between qubits and can be represented by basic unitary operators, i.e., quantum gates. The QFT is constructed using only H and CP gates.
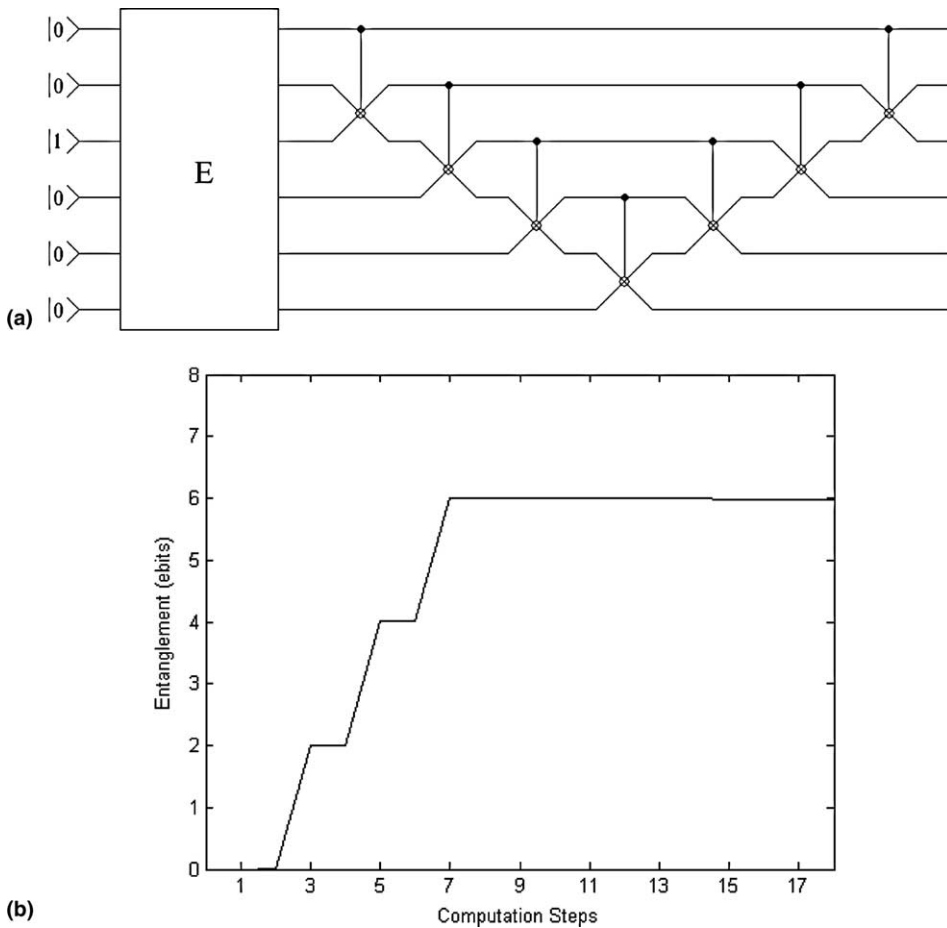

Fig. 11. (a) An entangled chain of six qubits followed by F gates. (b) Entanglement variation.

To construct the quantum circuit that performs QFT on an n-qubit QR a certain sequence of H and CP gates is applied. The index j counts the number of sequences and varies from $n-1$ down to 0. For the first sequence j is set equal to $n-1$ and the gate H is applied to the most significant bit, which is the $n-1$

$$(H_j), \quad j = n - 1. \tag{11}$$

In the second sequence j is reduced by one and the following gates are applied from the left to the right:

$$(CP_{j,n-1}H_j), \quad j = n - 2. \tag{12}$$

For the jth sequence the following gates are applied from the left to the right

$$(CP_{j,j+1}CP_{j,j+2} \ldots CP_{j,n-1}H_j). \tag{13}$$

The gates that are applied in all sequences are given by

$$(H_{n-1})(CP_{n-2,n-1}H_{n-2})(CP_{n-3,n-2}CP_{n-3,n-1}H_{n-3}) \cdots (CP_{0,1}CP_{0,2}CP_{0,3} \ldots H_0), \tag{14}$$

where, each parenthesis corresponds to one sequence and the sequences are applied and counted from the left to the right. The quantum circuit that executes the QFT is shown in Fig. 5.

QFT does not generate entanglement when applied to disentangled states. Here, the application of the QFT to entangled states will be studied. Fig. 6(a) shows a quantum computation where the second and third qubits are entangled by an H gate followed by a CN gate. After these two gates the four-qubit QFT circuit is applied. Fig. 6(b) shows the simulation of this computation. The entanglement variation is shown in Fig. 6(c). The H and CN gates generate entanglement equal to 2 ebits. The QFT increases the entanglement to about 3 ebits and then its value drops to 2.5 ebits and remains constant until the end of the computation.

Fig. 7(a) shows a quantum computation where the second and third qubits are entangled by an H gate followed by a CN gate. After these two gates the six-qubit QFT circuit is applied. Fig. 7(b) shows the simulation of this computation and the entanglement variation is shown in Fig. 7(c). The H and CN gates generate entanglement equal to 2 ebits. The QFT increases the entanglement to about 2.3 ebits and then its value drops to 1.5 ebits and remains constant until the end of the computation.

The simulation revealed that QFT changes the entanglement when applied to entangled states. After the application of the QFT the entanglement increases, then drops and remains constant until the end of the computation. In the case of computation of Fig. 6 the final entanglement is larger that the initial, whereas, in the case of Fig. 7 the final entanglement is smaller that the initial. This indicates that entanglement change by QFT is a subject worthy of further research.

4.3. Entangled chains

An entangled chain is formed when each qubit in the QR is entangled with its neighboring qubits. Entangled chains are important in modeling physical phenomena using quantum computers. Fig. 8(a) shows an entangled chain of six qubits and Fig. 8(b) the entanglement generation and variation caused by this chain.

In Fig. 9(a) the circuit of Fig. 8(a) is shown as a block with label "E". This figure shows an entangled chain followed by a configuration of CN gates. As shown in Fig. 9(b), the CN gates reduce the entanglement from 6 to 5 ebits at the fifteenth step. Fig. 10(a) shows an entangled chain followed by a configuration of CCN gates. As shown in Fig. 10(b) the entanglement varies slightly until the end of the computation. Fig. 11(a) shows an entangled chain followed by a configuration of F gates. Fig. 11(b) show that the application of F gates does not change the entanglement. The simulator presented here may prove to be a useful tool in studying entangled chains.

5. Conclusions

Entanglement generation and variation in several quantum computations was studied using a quantum computer simulator. The simulator was described and its block diagram was presented. The use of this simulator allowed the study of entanglement manipulation in quantum computations that comprise four and six qubits and a variety of quantum gates. Entanglement generation and variation in cases of repeated applications of quantum gate configurations and entangled chains followed by CN, CCN and F gates were simulated. The entanglement change caused by the QFT when applied to entangled states was also simulated. The simulator presented in this paper may become a useful tool for the study of entanglement generation and variation in quantum computations.

References

[1] A. Einstein, B. Podolsky, N. Rosen, Can quantum-mechanical description of physical reality be considered complete?, Physical Review 47 (1935) 777.
[2] C.P. Williams, S.H. Clearwater, Explorations in Quantum Computing, Springer, Berlin, 1998.
[3] G.P. Berman, G.D. Doolen, R. Mainieri, V.I. Tsifrinovich, Introduction to Quantum Computers, World Scientific, NJ, 1998.
[4] S. Hill, W.K. Wootters, Entanglement of a pair of quantum bits, Physical Review Letters 78 (1997) 5022.
[5] C.H. Bennett, D.P. DiVincenzo, J.A. Smolin, W.K. Wootters, Mixed-state entanglement and quantum error correction, Physical Review A 54 (1996) 3824.
[6] P. Shor, Algorithms for quantum computation: discrete logarithms and factoring, in: Proceedings of the 35th Annual Symposium on Foundations of Computer Science, 1994, p. 124.
[7] R.V. Ramos, Numerical algorithms for use in quantum information, Journal of Computational Physics 192 (2003) 95.
[8] V. Vedral, M.B. Plenio, Entanglement measures and purification procedures, Physical Review A 57 (1998) 1619.
[9] K. Audenaert, J. Eisert, M.B. Plenio, Entanglement properties of the harmonic chain, Physical Review A 66 (2002) 042327-1.
[10] R.V. Ramos, R.F. Souza, Calculation of the quantum entanglement measure of bipartite states, based on relative entropy, using genetic algorithms, Journal of Computational Physics 175 (2002) 576.
[11] J. Batle, A.R. Plastino, M. Casas, A. Plastino, On the distribution of entanglement changes produced by unitary operations, Physics Letters A 307 (2003) 253.
[12] J. Batle, M. Casas, A. Plastino, A.R. Plastino, The statistics of the entanglement generated by the Hadamard–CNOT quantum circuit, Physica A 327 (2003) 140.
[13] I.G. Karafyllidis, Visualisation of the quantum Fourier transform using a quantum computer simulator, Quantum Information Processing 2 (2003) 271.
[14] I.G. Karafyllidis, Cellular quantum computer architecture, Physics Letters A 320 (2003) 35.
[15] R. Jozsa, Quantum factoring, discrete logarithms, and the hidden subgroup problem, Computing in Science and Engineering 3 (2001) 34.
[16] A.O. Pittenger, An Introduction to Quantum Computing Algorithms, Birkhauser, Berlin, 2000.
[17] Y.S. Weinstein, M.A. Pravia, E.M. Fortunato, S. Lloyd, D.G. Cory, Implementation of the quantum Fourier transform, Physical Review Letters 86 (2001) 1889.
[18] A. Ekert, R. Jozsa, Quantum computation and Shor's factoring algorithm, Reviews of Modern Physics 68 (1996) 733.